Biocybernetics and Biomedical Engineering 44 (2024) 304–311

Contents lists available at ScienceDirect

Biocybernetics and Biomedical Engineering

journal homepage: www.elsevier.com/locate/bbe

Research Paper

# Prediction of central nervous system oxygen toxicity symptoms using electrodermal activity and machine learning

Md-Billal Hossain [a,1], Kia Golzari [a,1], Youngsun Kong [a], Bruce J. Derrick [b,c], Richard E. Moon [b,c], Michael J. Natoli [b], M. Claire Ellis [b,c], Christopher Winstead-Derlega [b,c], Sara I. Gonzalez [b], Christopher M. Allen [b,c], Mathew S. Makowski [b,c], Brian M. Keuski [d], John J. Freiberger [c], Hugo F. Posada-Quintero [a], Ki H. Chon [a,*]

[a] Department of Biomedical Engineering, University of Connecticut, Storrs, CT, USA
[b] Division of Emergency Medicine, Duke University, Durham, NC, USA
[c] Department of Anesthesiology, Duke University, Durham, NC, USA
[d] United States Navy, USA

ARTICLE INFO

*Keywords:*
Seizure prediction
oxygen toxicity
Electrodermal activity
Machine learning

ABSTRACT

*Objective:* Breathing elevated oxygen partial pressures ($PO_2$) prior to SCUBA diving increases the risk of developing central nervous system oxygen toxicity (CNS-OT), which could impair performance or result in seizure and subsequent drowning. We aimed to study the dynamics of electrodermal activity (EDA) while breathing elevated $PO_2$ in the hyperbaric environment ($HBO_2$) as a possible means to predict impending CNS-OT. To this end, we used machine learning to automatically detect and predict the onset of symptoms associated with CNS-OT in humans by using features derived from EDA in both time and frequency domains.

*Methods:* We collected electrodermal activity (EDA) data from forty-nine exposures to $HBO_2$ while subjects were undergoing cognitive load and exercise in a hyperbaric oxygen chamber. Four independent experts were present during the experiment to monitor and classify any symptoms associated with hyperbaric oxygen toxicity. We computed a highly sensitive time varying spectral EDA index, named TVSymp, and extracted informative features from skin conductance responses (SCRs). Machine learning algorithms were trained and validated for classifying features from SCRs and TVSymp as CNS-OT related or non-CNS-OT related. Machine learning models were validated using a subject-independent leave one subject out (LOSO) validation scheme.

*Results:* Our machine learning model was able to classify EDA dynamics related to CNS-OT with 100 % sensitivity and 84 % specificity via LOSO validation. Moreover, the median prediction time for CNS-OT symptoms was ~ 250 s preceding the occurrence of actual symptoms.

*Significance:* This study shows that EDA can potentially be used for early prediction of CNS-OT in divers with a high sensitivity and sufficient prediction time for countermeasures. While the study results are promising, independent validation datasets are warranted to confirm the findings. However, the current results are well corroborated in an animal study, which consistently showed seizure prediction time of 2 min prior to seizure.

## 1. Introduction

Hyperbaric oxygen ($HBO_2$) therapy has been used for treatment of disorders such as carbon monoxide toxicity (CO) [1], decompression sickness [2], and treating wounds [3,4]. Hyperbaric oxygen therapy ($HBO_2T$) exposes human body to 100 % oxygen ($O_2$) at ambient pressure higher than one atmosphere (1 ATM) [5]. The ambient pressure in hyperbaric chambers can be increased to partial pressures of oxygen ($PO_2$) exceeding 1 ATA because reactive oxidative species (ROS) and hydrostatic effects can improve wound healing and affect the bubble sizes in decompression sickness caused by high partial pressure of nitrogen ($N_2$) [6].

Even though the toxic nature of oxygen is usually overlooked, there are several side effects of $HBO_2T$ including $HBO_2$-induced seizure [7].

* Corresponding author at: Department of Biomedical Engineering, University of Connecticut, Storrs, CT 06269, USA.
*E-mail address:* Ki.chon@uconn.edu (K.H. Chon).
[1] Authors contributed equally.

https://doi.org/10.1016/j.bbe.2024.03.004
Received 20 October 2023; Received in revised form 3 March 2024; Accepted 20 March 2024
Available online 27 March 2024

Divers who are treated using prolonged hyperbaric oxygen exposure are very likely to develop symptoms related to $HBO_2$ toxicity. Prolonged exposure to elevated $PO_2$ increases the risk of both pulmonary and central nervous system oxygen toxicity (CNS-OT), which is characterized by decrease in pulmonary function, chest tightness, dyspnea, cough, headache, diaphoresis, nausea, tinnitus, lip twitching, and so on. Thus, autonomic nervous system activity, more specifically, sympathetic activity, known to be elevated during the above-noted symptoms, can be a potential tool to predict CNS-OT symptoms.

The risk of central nervous system oxygen toxicity is proportional to both partial pressure of oxygen ($PO_2$) and exposure time. The higher the $PO_2$, the higher the risk of CNS-OT [8]. Typically, 2–3 ATA is considered the threshold for CNS-OT risk, however, this could be even lower depending on concurrent activities such as exercise or cognitive load, and immersion [4,6]. Therefore, to maximize the potential benefits of $HBO_2$T, determining the oxygen toxicity mechanisms and early prediction of $HBO_2$ toxicity symptoms are essential.

Our recent studies involving animals and human subjects breathing $HBO_2$ in a hyperbaric chamber have shown consistent seizure activities (in the animals) and symptoms related to oxygen toxicity due to CNS-OT induced by $HBO_2$ [9,10]. As seizures are associated with elevated sympathetic activity [9], a quantitative measure of sympathetic activity could be used to predict and detect seizure and its related symptoms.

Electrodermal activity (EDA) has recently become a popular noninvasive surrogate measure of sympathetic activity, and has been used in diverse applications such as stress and pain detection [11–17], autism examination [18,19], panic disorder studies [20], detection of depression [21], and recognition of emotional states [22,23]. EDA measurements are collected by placing an electrode on each of two fingers, then injecting a small constant current through the electrodes and measuring the corresponding change in electrical conductance between the electrodes[24,25].

Typically, EDA analysis is performed in the time domain by decomposing the signal into phasic and tonic components [26], where the tonic components represent the overall trend of the EDA and the phasic components represent skin conductance responses (SCRs) (shown in Fig. 1), which have faster dynamics and more visibly discernable responses than do the tonic components. While several studies used these time-domain features, some studies reported reproducibility issues with them [26–28].

Recently, our lab has developed a sensitive and consistent measure of EDA called the time-varying sympathetic (TVSymp) index [29], using time-varying spectral analysis. TVSymp characterizes the EDA signal components in the frequency band between 0.08 and 0.25 Hz in humans. TVSymp has been used successfully in different EDA applications, including stress during sleep deprivation [30] and pain detection [27,31].

A recent study on rats from our group has shown that there are large increases in TVSymp amplitudes on average 1.9 min before $HBO_2$-induced seizures in rats [32]. We also observed significant increase in TVSymp amplitudes ~ 1 min prior to manifestation of CNS-OT symptoms in humans [26]. However, the specificity of symptom prediction was low (67 % specificity) in humans. Given that machine learning is adept at unraveling complex nonlinear patterns, we hypothesized that machine learning algorithms can potentially lead to better performance metrics in predicting symptoms related to CNS-OT in humans.

To this end, we computed features from the individual SCRs and TVSymp-derived indices and applied a machine learning classifier to differentiate between “no symptoms” and “symptoms associated with CNS-OT.” The machine learning classification yielded 100 % sensitivity and 84 % specificity in classifying CNS-OT related symptoms. Preliminary results of this study were presented at the IEEE EMBC conference in 2022 [26]. The conference paper contains a small portion of the dataset and limited analysis, while this paper includes data from a larger number of subjects with comprehensive details on the protocols with rigorous signal analysis and machine learning results.

## 2. Materials and Methods

### 2.1. Description of dataset

Our dataset consists of simultaneously collected EDA and electrocardiogram (ECG) from 26 male subjects aged between 20 and 48 years of age. While every subject was expected to complete two exposures to $HBO_2$, only twenty-three subjects completed both exposures, and three subjects completed one exposure. Thus, a total of forty-nine exposures were considered for this study.

The experimental protocol was approved by Duke University’s Institutional Review Board and all volunteers executed a written informed consent form to participate in the study. The experiments were performed in the “foxtrot” chamber pool (as shown in Fig. 2) at the Duke University Hyperbaric Center, Duke University Hospital. During the experiment, subjects were immersed in 28 ± 1 °C water up to the shoulders, breathing 100 % O2 at 35 feet of seawater (oxygen partial pressure 2.06 ATA). Additionally, subjects exercised on an underwater cycle ergometer at approximately 100 W output and performed NASA’s Multi-Attribute Task Battery-II (MATB-II) [33] cognitive tests. The exposure lasted for a maximum duration of 120 min or until symptoms of CNS-OT were observed. For safety purposes, subjects were seated in water in a head-out position to avoid head submersion in the event of convulsion or loss of consciousness. We were able to rapidly, and safely, identify symptoms of oxygen toxicity by conducting this study one subject at a time. Convulsions are often preceded by warning signs, which were meticulously monitored by the safety diver in the water with

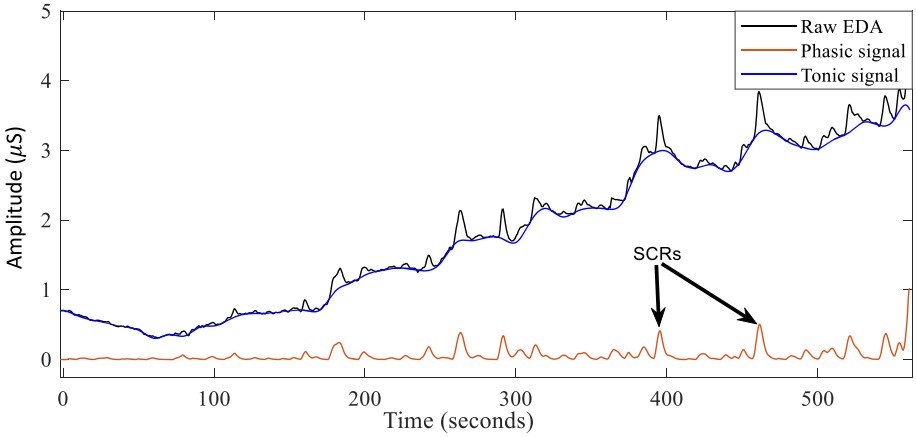


**Fig. 1.** Example of EDA record and its components.

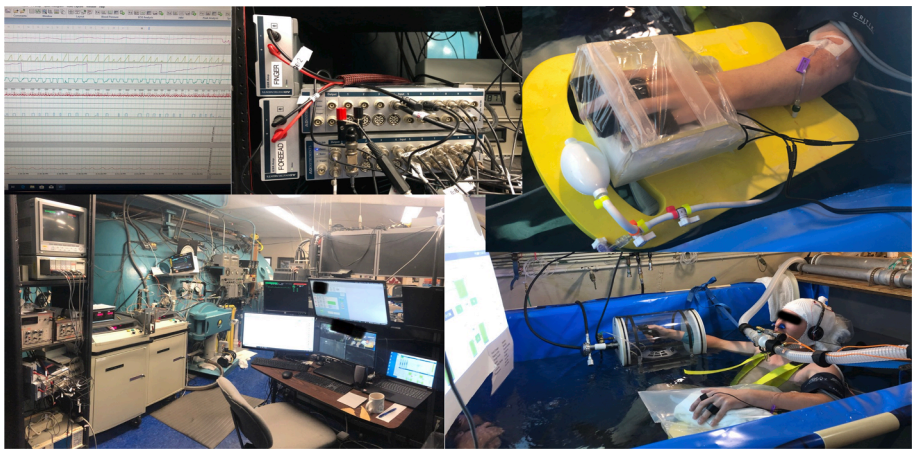

**Fig. 2.** Experimental setup for data collection.

the subject. The protocol was terminated (exercise stopped, subject switched from 100 % oxygen to chamber air simply by removing the subject's mouthpiece) upon the occurrence of ANY symptom, or a sudden decrease in cognitive performance on the MATB-II, or identification of EEG waveforms indicative of seizure or impending seizure. Some of the notable signs of CNS-OT include visual disturbances, headache, diaphoresis, nausea, tinnitus, twitching or tingling of the face or limbs. Due to potential harm to subjects and per the IRB regulations, any immediate signs of symptoms related to oxygen toxicity led to stoppage of the experiments. Hence, all symptoms were ranked equally and any appearance of them resulted in immediate stoppage of the experiment. This is the reason why, in some cases, it was not crystal clear if oxygen toxicity symptoms occurred, therefore, the experts rated these as probable.

EDA and ECG signals were collected simultaneously at a sampling frequency of 100 Hz. EDA was collected using dry (no-hydrogel) stainless-steel electrodes and using galvanic skin response module FF116 (ADInstruments, Sydney, Australia) while ECG signals were collected using Ag/AgCl electrodes and a Hewlett-Packard ECG monitor (Palo Alto, CA, USA).

Each exposure was annotated by four independent experts as "definite" CNS-OT, "probable" CNS-OT, or "non-CNS-OT" which is when subjects either did not exhibit any symptoms or their symptoms were concluded by experts to be not associated with CNS-OT. Finally, a majority voting poll was used to create the final adjudication. In the case of 50/50 decision splits (two annotations as "definite" and two as "probable"), the exposure was labeled as "probable." Hence, we have eighteen "Definite CNS-OT," thirteen "Probable," and eighteen "non-CNS-OT" labeled exposures.

### 2.2. EDA signal processing

#### 2.2.1. Preprocessing

Like most biosignals, EDA can be affected by occasional motion artifacts (MA), which may result in lower specificity for detecting CNS-OT [34,35]. A previous study used an automatic MA detection algorithm [36] for detecting MA in EDA signals and excluded detected MA segments from the analysis. However, this method was developed using a different dataset that was not related to CNS-OT detection, hence, its performance on this CNS-OT dataset was suboptimal. For more reliable results, MA should be removed from the analysis since MA can be misinterpreted as peaks corresponding to the presence of CNS-OT. Therefore, we used annotations from three independent EDA experts and applied a majority voting scheme to separate segments with MA from clean segments. A median filter (one second window) and a low pass finite impulse response filter with a cut-off-frequency of 1 Hz were applied to remove high frequency content of the signal.

#### 2.2.2. Time-varying spectral analysis of EDA: TVSymp

TVSymp, which uses a time-varying spectral analysis approach, has been successfully applied in diverse applications involving stress, pain, fatigue, and dehydration detection [27,28,37] as these cases all involve increased sympathetic innervation. TVSymp has been found to be less intra-subject variant and more sensitive when compared to the time-domain measures of EDA (i.e., tonic and phasic components).

TVSymp calculation involves decomposition of the EDA signal into multiple frequency bands using a high resolution time–frequency decomposition called variable frequency complex demodulation (VFCDM) [38]. VFCDM provides both high time and frequency resolution, while retaining accurate amplitude distribution of the signal. This method then uses only the frequency bands within the range of $0.08-0.25Hz$ to reconstruct the signal. Finally, an envelope of the instantaneous amplitude of the signal is computed using the Hilbert transform [39]. This sequence of computations is described using the following equations.

The original EDA signal $y(t)$ can be expressed as a summation of N (=12 in our case) different VFCDM components as follows:

$$y(t) = \sum_{i=1}^{N} C_i(t) \tag{1}$$

where $C_i$ represents the *ith* VFCDM component. Considering a sampling frequency of $2Hz$ and 12 equally divided sub bands, components 2–3 contain the frequency range $0.08-0.25Hz$. Thus, we reconstruct the EDA signal $y'(t)$ by summing components 2 and 3 of the VFCDM decomposition:

$$y'(t) = C_2(t) + C_3(t) \tag{2}$$

we then compute the envelope of the signal $y'(t)$ using the Hilbert transform. An analytic signal, $A(t)$ of the $y'(t)$, can be expressed as follows:

$$A(t) = y'(t) + jY'(t) \tag{3}$$

where $Y'(t)$ is the Hilbert transform of the original signal $y'(t)$ which can be obtained by the following equation:

$$Y'(t) = \frac{1}{\pi} P \int_{-\infty}^{\infty} y'(\tau)/(t-\tau)d\tau \tag{4}$$

where P refers to the Cauchy principal value.

The instantaneous amplitude and phase of the analytic signal $A(t)$ can be obtained as below.

$$a(t) = \left[y'^2(t) + Y'^2(t)\right]^{1/2} \tag{5}$$

$$\theta(t) = arctan(Y^{'}(t)/y^{'}(t)) \quad (6)$$

The instantaneous amplitude $a(t)$ is considered the TVSymp time series. Fig. 3 shows the representative TVSymp time series for a'CNS-OT' and a 'No Symptom' subjects.

As shown in Fig. 3, preceding CNS-OT symptoms, there are significant increases in TVSymp amplitudes. Annotations for MA are also plotted (thick red rectangular box) to designate large TVSymp amplitudes due to the MA. For non-CNS-OT there is no significant sudden rise in TVSymp values as compared to the CNS-OT case.

### 2.3. Data preparation for Machine learning

Our previous study reported significant and sudden increase in TVSymp amplitudes preceding the CNS-OT symptoms compared to the first five minutes (baseline) of the recording, where we would not expect to have any CNS-OT symptoms. However, for more accurate and automated prediction of seizures, we analyzed the entire data recording to identify the earliest possible onset of the sudden and large increases in TVSymp amplitudes prior to the experts' adjudication of when CNS-OT related symptoms occurred.

Based on our observations, TVSymp amplitudes increase significantly preceding CNS-OT related symptoms. Moreover, during the first five minutes there were no seizure-related activities, as we did not observe any sudden and large increase in TVSymp amplitudes. This observation is buttressed by the histogram shown in Fig. 4, which shows TVSymp amplitudes in both the last (for those defined as 'CNS-OT' subjects) and first five minutes of EDA. For the first five minutes, 95 % of TVSymp amplitudes are less than ~ 4. However, in the last five minutes of the recordings (for CNS-OT subjects only) TVSymp amplitudes far exceed 4 and in some cases they are as large as 19 when symptoms of CNS-OT tend to occur.

#### 2.3.1. Feature extraction

We computed 4 different features from each of the SCRs, including peak TVSymp amplitude, rising and falling slopes of the SCRs, and width of the SCRs.

### 2.4. Machine learning

We examined multiple machine learning classifiers, including linear discriminant analysis (LDA), logistic regression, linear support vector machine (SVM), decision tree, random forests, and gradient boosting classifiers. Since we have a limited dataset, we used a subject-independent leave-one-subject-out (LOSO) validation strategy to evaluate our machine learning models. We computed sensitivity and specificity by averaging the predictions from each test fold.

#### 2.4.1. Data balancing

After annotation, a total of 217 samples were related to CNS-OT and 9100 samples were not related to CNS-OT. Thus, we have a highly imbalanced dataset with more negative samples. Therefore, to avoid biased training, we used the synthetic minority oversampling technique (SMOTE) [40] to oversample the examples in the minority class.

#### 2.4.2. Hyperparameter optimization

For each fold of the LOSO validation, we optimized the hyper parameters of the classifiers using the grid-search cross-validation technique with group K-fold (k = 5) cross validation on the training data. For linear SVM, we varied the parameter $C$ from 0.01 to 1000 using multiples of 100. For random forests and gradient boosting classifiers, we varied the maximum depth of the trees from 3 to 6, and the number of estimators between 40 and 100 with a step size of 20.

#### 2.4.3. Training Machine learning algorithms

To train the machine learning algorithms, we only used the first and last five minutes of the data, as supported by the histogram plot shown

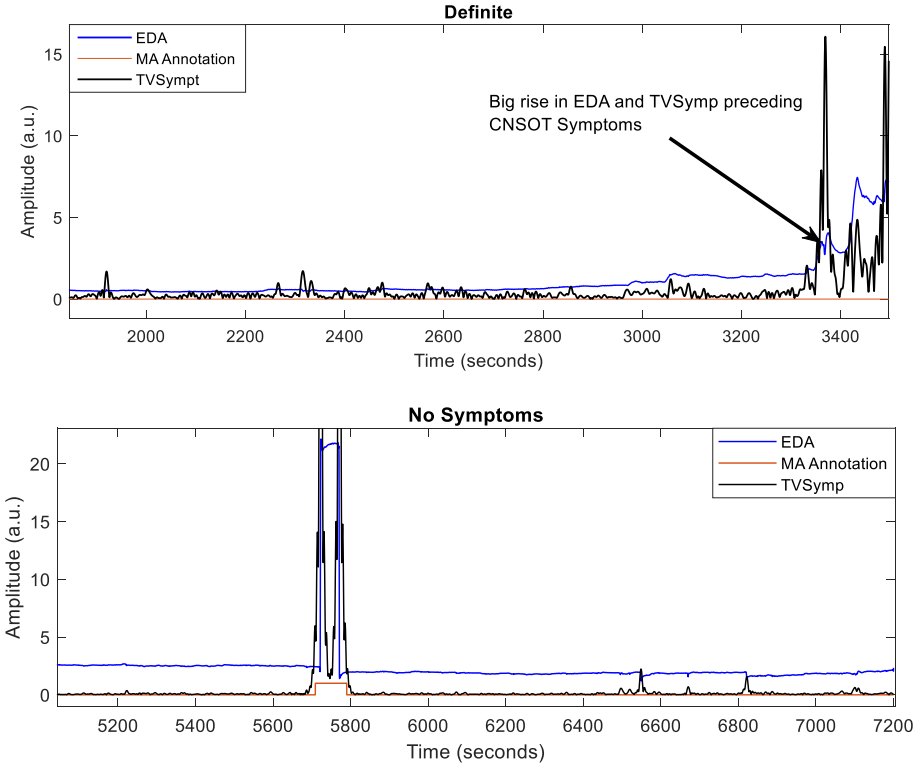


**Fig. 3.** Representative examples of EDA and the corresponding TVSymp for CNS-OT and non CNS-OT exposures. The thick rectangular red line represents motion artifact detection using our algorithm.

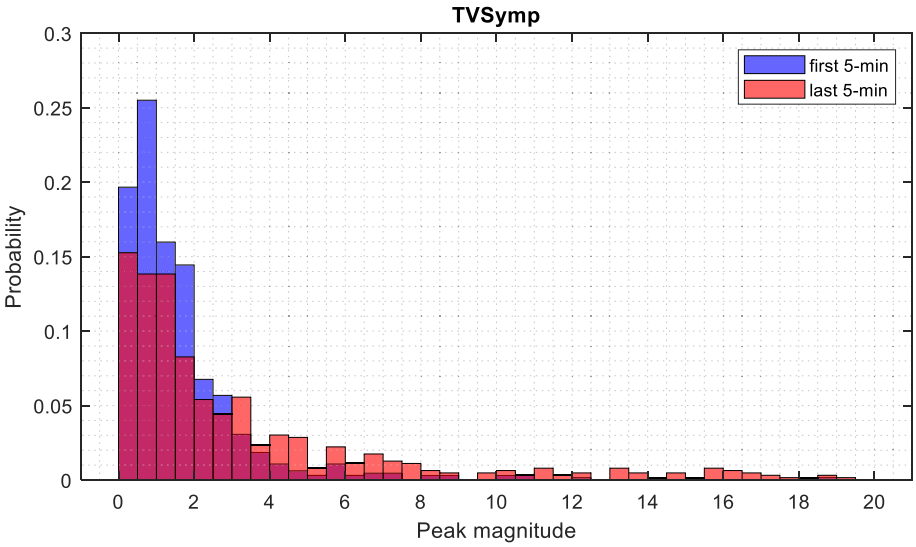


**Fig. 4.** Histogram of TVSymp peaks in the first and last five minutes of EDA recordings.

in Fig. 4. However, note that for validation we considered data from the entire exposure to assess how early our model detects symptoms associated with CNS-OT.

## 3. Results

For evaluating the machine learning models, we used the LOSO validation strategy and compared the ML models in terms of sensitivity and specificity, which are defined as:

$$Sensitivity = \frac{TP}{TP + FN} \tag{7}$$

$$Specificity = \frac{TN}{TN + FP} \tag{8}$$

where, $TP, TN, FP, andFN$ represent the number of true positive, true negative, false positive, and false negative samples, respectively. In our case, the positive class represents SCRs related to CNS-OT symptoms and the negative class represents no symptoms associated with CNS-OT.

As previously mentioned, each experimental session was annotated by four independent experts, and we considered majority voting for the final adjudicated labeling. However, for some symptomatic cases, half of the experts labeled the symptoms as "Definite CNS-OT" and the other half were unsure, hence, these cases were labeled as "Probable." At first, we excluded all the probable cases, however, most of them had similar EDA signatures as "Definite CNS-OT." Given that we have limited data samples for CNS-OT, additional positive cases of CNS-OT are beneficial for better training of machine learning models. Hence, we included cases with "Probable" CNS-OT in the CNS-OT cases, when at least two experts ($\geq$50 %) annotated them as "Definite CNS-OT." This led to an additional seven definite CNS-OT cases. However, we report results by including and excluding probable cases, as shown in Table 1.

Table 1 summarizes the machine learning results on predicting CNS-OT associated symptoms. We considered six different machine learning models, as listed in the table. The table shows results for both regular labeling without including "Probable" symptoms and including $\geq$ 50 % "Probable" CNS-OT symptoms. Almost all of the machine learning models provided improved performance after including the $\geq$ 50 % "Probable" subjects.

The linear SVM showed the maximum sensitivity of 98.84 % with a good specificity of 81.40 %. However, the performance of the linear SVM did not improve significantly after adding probable cases. Even though LDA provided high specificity, the sensitivity was much lower than for the other classifiers. The logistic regression classifier provided more consistent results both before and after including $\geq$ 50 % "Probable" data; for the latter case, it showed 100 % sensitivity with 82.13 % specificity. The performance of the tree-based algorithms such as the decision tree, random forests, and gradient boosting classifiers, were comparable; all of them showed improved results after including probable cases of CNS-OT. In order to evaluate individual feature's importance, we used permutation feature importance technique [41,42], which measures the contribution of each feature to the statistical performance of a fitted model. The feature importance score for the SCR width, rising time, falling time, and the TVsymp amplitude were ($mean \pm std$) $0.0009 \pm 0.003$, $0.0167 \pm 0.003$, $0.0131 \pm 0.002$, and $0.2564 \pm 0.009$ respectively. This suggests that the TVsymp amplitude is the most important feature out of the four features used by the model.

**Table 1**
Machine Learning Results on seizure detection.

| Excluding "Probable" | Classifier | Sensitivity | Specificity |
|---|---|---|---|
| | LDA | 74.42 | **89.61** |
| | SVM (linear) | **98.84** | 81.40 |
| | Logistic Regression | 98.26 | 82.97 |
| | Decision Tree | 87.79 | 83.98 |
| | Random Forest | 91.86 | 83.98 |
| | Gradient Boosting | 94.77 | 83.00 |
| Including $\geq$ 50 % "definite" | LDA | 80.51 | **86.49** |
| | SVM (linear) | 97.88 | 83.28 |
| | Logistic Regression | **100** | 82.13 |
| | Decision Tree | 95.33 | 83.27 |
| | Random Forest | 95.33 | 83.27 |
| | Gradient Boosting | 96.61 | 82.65 |

The fact that the machine classifiers' performance improved after including probable cases can be visualized from EDA characteristics. For example, Fig. 5 shows TVSymp series for a representative "definite" CNS-OT case and a "Probable" case. As shown in Fig. 5, both cases showed a sudden and significant rise in the TVSymp signal, which is the key signature for CNS-OT symptoms, in our observation, albeit the amplitudes in the definite CNS-OT case were much greater than in the probable CNS-OT case. Given the limited number of definite CNS-OT cases, and the fact that probable CNS-OT cases have similar significant increases in amplitudes of TVSymp values compared to baseline, our decision to include more data from training and testing is justified and consequently led to better classification results.

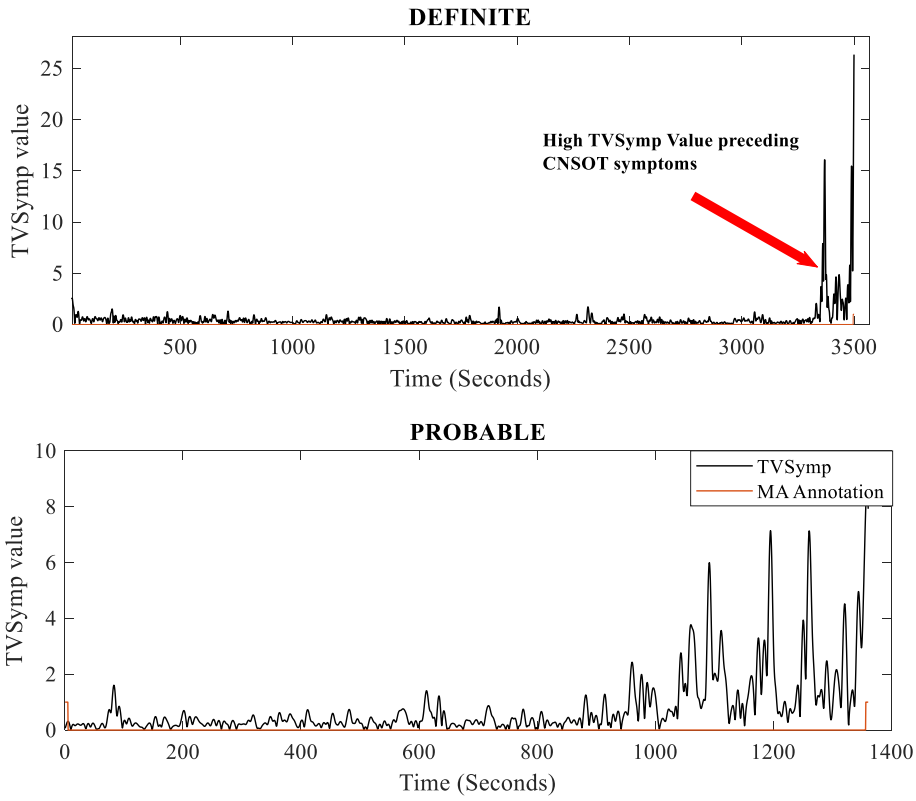


**Fig. 5.** TVSymp characteristics for "Definite" CNS-OT exposure and $\geq$ 50 % "Probable" exposure.

### 3.1. Prediction time

We computed the prediction time of CNS-OT symptoms by considering the first significant increase in TVSymp detected as CNS-OT. The median prediction time as shown in Fig. 6, is slightly above 250 s while the 95 % confidence interval around the mean is $199 \pm 98 (mean \pm sd)$. This suggests that prediction of CNS-OT symptoms can be on average 200 s preceding the symptoms, which is greater than 4 min.

## 4. Discussion

This work is one of the first studies about prediction of CNS-OT symptoms in humans using EDA signals. The performance of the machine learning models showed promising results. The study outcome corroborates our recent findings in which we also observed significant increase in EDA activity prior to onset of seizures in rats undergoing $HBO_2$ exposure [32]. Specifically, there were significant and sudden increases in TVSymp amplitudes $>$ 2 min preceding seizure onset; the onset was verified via both EEG and video recordings of seizure-related convulsions in the rats. The rats were exposed to $HBO_2$ at 5 ATA and sudden decompression led to seizures in all 10 rats. Hence, the sensitivity and specificity were both found to be 100 %. However, for ethical and safety reasons for humans, the partial pressure of oxygen in this study was not increased beyond 2 ATA, and the subjects were removed from the experimental chamber as soon as mild symptoms associated with CNS-OT appeared. Hence, for the current work, prediction was based on the presence of symptoms associated with CNS-OT rather than predicting seizures. Since symptoms related to CNS-OT are precursors to

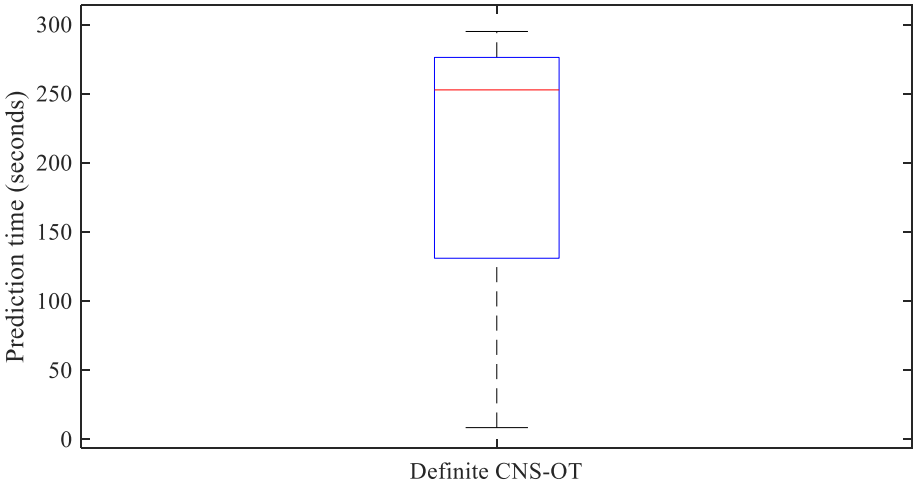


**Fig. 6.** Prediction time using machine learning (the redline shows the median value).

seizures, it is reasonable to expect that our prediction time would be even longer before actual seizures. When comparing humans to rats, however, we did find a greater prediction time opportunity before the appearance of symptoms associated with CNS-OT in humans than seizures in rats. The average prediction time was $> 3$ min in humans before symptoms associated with CNS-OT, whereas the average prediction time was $\sim 2$ min in rats before the onset of seizures. Approximately 3 min of warning time is sufficient for preparation of countermeasures such as alerting dive buddies and alerting the diver of impending seizures.

While this study presented evidence for prediction of CNS-OT symptoms in humans, there are some limitations of this study. First, because of the limited dataset, the machine learning models could not be validated on an independent dataset. Also, the fact that including more subjects (e.g., including probable CNS-OT cases) improved the classification for most of the machine learning models, shows that more diverse sets of training data for machine learning models can lead to better characterization of the signal dynamics to discriminate SCRs that correspond to CNS-OT symptoms. Therefore, more validation using other independent datasets is necessary to further confirm the results of this study.

Another possible limitation of the dataset is the annotation of EDA. While we conservatively assumed that EDA disturbances in the last five minutes were related to the CNS-OT symptoms, in reality, we do not know when an EDA signal exhibits CNS-OT signatures. Thus, EDA activities immediately before the last five minutes may be related to the CNS-OT symptoms as well, which could be one of the reasons for our relatively low specificity.

Moreover, we used manual annotations for discarding data segments with motion artifacts, to provide more reliable and accurate prediction of CNS-OT symptoms. While manually discarding motion artifacts gives us the opportunity to train our machine learning models using more reliable signals, this is not suitable for an automated approach to predict CNS-OT symptoms in real time. For automated applications, we are planning to apply our recently developed automatic motion artifact detection and removal algorithms [34,35]. However, both algorithms may require additional training data to fully compensate for all possible scenarios involving motion artifacts, especially in water immersion. Currently, we are developing hardware to collect EDA data from the feet of divers, as the foot was found to be the best alternate location for EDA data collection when palmer sites are not available [43]. In addition, we will be implementing our machine learning model for CNS-OT detection along with automatic motion artifact detection and correction into the device to provide early warning of CNS-OT.

Despite some limitations, this study showed the efficacy of machine learning in predicting symptoms associated with CNS-OT nearly 3 min in advance, to provide necessary warnings to the diver of possible impending seizures. Such impressive early prediction of symptoms associated with CNS-OT in humans has not been demonstrated prior to our current study.

**Ethical and integrity policies**.

**Ethics and patient consent approval statement**.

The human study was approved by Duke University's IRB and human consent was received prior to experiments.

**Key points:**

- Breathing elevated oxygen partial pressures ($PO_2$) prior to SCUBA diving increases the risk of developing central nervous system oxygen toxicity (CNS-OT).
- Our work shows that CNST-OT symptoms can be predicted $> 4$ min prior to actual symptoms.
- Machine learning using EDA features showed CNS-OT discrimination with 100 % sensitivity and 84 % specificity.

## CRediT authorship contribution statement

**Md-Billal Hossain:** Data curation, Formal analysis, Investigation, Methodology, Validation, Writing – original draft, Writing – review & editing. **Kia Golzari:** Data curation, Formal analysis, Investigation. **Youngsun Kong:** Methodology, Validation, Writing – original draft, Writing – review & editing. **Bruce J. Derrick:** Funding acquisition, Supervision, Project administration, Data curation, Validation, Writing – original draft, Writing – review & editing. **Richard Moon:** Validation, Writing – original draft. **Michael J. Natoli:** Data curation. **M. Claire Ellis:** . **Christopher Winstead-Derlega:** Data curation. **Sara I. Gonzalez:** Data curation. **Christopher M. Allen:** Data curation. **Mathew S. Makowski:** Data curation. **Barian M. Keuski:** Data curation. **John J. Freiberger:** Funding acquisition, Data curation, Validation, Writing – original draft, Writing – review & editing. **Hugo F. Posada–Quinteroalidation:** Writing – original draft, Writing – review & editing. **Ki Chon:** Conceptualization, Funding acquisition, Investigation, Methodology, Project administration, Resources, Supervision, Validation, Writing – original draft, Writing – review & editing.

## Declaration of Competing Interest

The authors declare that they have no known competing financial interests or personal relationships that could have appeared to influence the work reported in this paper.

## Acknowledgment

This work was supported by the Office of Naval Research grant N00014-21-1-2255.

## References

[1] Pace N, Strajman E, Walker EL. Acceleration of Carbon monoxide elimination in man by high pressure oxygen. Sci 1950;111:652–4. https://doi.org/10.1126/science.111.2894.652.
[2] United States: Defense Department: Navy Department: Naval Sea Systems Command, United States: Naval Sea Systems Command,. U.S. Navy Diving Manual. Revision 7. Defense Department; 2016.
[3] Thom SR. Hyperbaric oxygen – its mechanisms and efficacy. Plast Reconstr Surg 2011;127:131S–S141. https://doi.org/10.1097/PRS.0b013e3181fbe2bf.
[4] Kranke P, Bennett MH, James M-M-S, Schnabel A, Debus SE, Weibel S. Hyperbaric oxygen therapy for chronic wounds. Cochrane Database Syst Rev 2015. https://doi.org/10.1002/14651858.CD004123.pub4.
[5] Ortega MA, Fraile-Martinez O, García-Montero C, Callejón-Peláez E, Sáez MA, Álvarez-Mon MA, García-Honduvilla N, Monserrat J, Álvarez-Mon M, Bujan J, Canals ML. A General Overview on the Hyperbaric Oxygen Therapy: Applications, Mechanisms and Translational Opportunities. Medicina (Kaunas). 2021 Aug 24;57(9):864. doi: 10.3390/medicina57090864. PMID: 34577787; PMCID: PMC8465921.
[6] Manning, Edward P. "Central Nervous System Oxygen Toxicity and Hyperbaric Oxygen Seizures." Aerospace Medicine and Human Performance 87, no. 5 (May 1, 2016): 477–86. https://doi.org/10.3357/AMHP.4463.2016.
[7] Plafki C, Peters P, Almeling M, Welslau W, Busch R. Complications and side effects of hyperbaric oxygen therapy. Aviat Space Environ Med 2000;71:119–24.
[8] Jenkinson SG. Oxygen toxicity. New Horiz 1993;1:504–11.
[9] Wannamaker BB. Autonomic nervous system and epilepsy. Epilepsia 1985;26:S31–9. https://doi.org/10.1111/j.1528-1157.1985.tb05722.x.
[10] Freeman R, Chapleau MW. Chapter 7 - testing the autonomic nervous system. In: Said G, Krarup C, editors. Handbook of Clinical Neurology, vol. 115. Elsevier; 2013. p. 115–36. https://doi.org/10.1016/B978-0-444-52902-2.00007-2.
[11] Hernandez J, Morris RR, Picard RW. Call center stress recognition with person-specific models. In: D'Mello S, Graesser A, Schuller B, Martin J–C, editors. Affective Computing and Intelligent Interaction. Berlin, Heidelberg: Springer; 2011. p. 125–34. https://doi.org/10.1007/978-3-642-24600-5_16.
[12] Gjoreski M, Gjoreski H, Luštrek M, Gams M. Continuous stress detection using a wrist device: in laboratory and real life. Proceedings of the 2016 ACM International Joint Conference on Pervasive and Ubiquitous Computing: Adjunct, New York, NY, USA: Association for Computing Machinery; 2016 1185 93. DOI: 10.1145/2968219.2968306.
[13] Healey J, Nachman L, Subramanian S, Shahabdeen J, Morris M. Out of the lab and into the fray: Towards modeling emotion in everyday life. In: Floréen P, Krüger A, Spasojevic M, editors. Pervasive Computing. Berlin, Heidelberg: Springer; 2010. p. 156–73. https://doi.org/10.1007/978-3-642-12654-3_10.
[14] Setz C, Arnrich B, Schumm J, Marca RL, Tröster G, Ehlert U. Discriminating stress from cognitive load using a Wearable EDA Device. IEEE Trans Inf Technol Biomed 2010;14:410–7. https://doi.org/10.1109/TITB.2009.2036164.
[15] Momin A, Bhattacharya S, Sanyal S, Chakraborty P. Visual attention, mental stress and gender: a study using physiological signals. IEEE Access 2020;8:165973–88. https://doi.org/10.1109/ACCESS.2020.3022727.

[16] Kong Y, Posada-Quintero HF, Chon KH. Pain Detection using a Smartphone in Real Time*. 2020 42nd Annual International Conference of the IEEE Engineering in Medicine Biology Society (EMBC), 2020 4526 9. DOI: 10.1109/EMBC44109.2020.9176077.
[17] Kong Y, Posada-Quintero H, Chon K. Sensitive physiological indices of pain based on differential characteristics of electrodermal activity. IEEE Trans Biomed Eng 2021:1. https://doi.org/10.1109/TBME.2021.3065218.
[18] Prince EB, Kim ES, Wall CA, Gisin E, Goodwin MS, Simmons ES, et al. The relationship between autism symptoms and arousal level in toddlers with autism spectrum disorder, as measured by electrodermal activity. Autism 2017;21:504–8. https://doi.org/10.1177/1362361316648816.
[19] Schupak BM, Parasher RK, Zipp GP. Reliability of electrodermal activity: quantifying sensory processing in children with autism. Am J Occup Ther 2016;70:1–6. https://doi.org/10.5014/ajot.2016.018291.
[20] Wendt J, Lotze M, Weike AI, Hosten N, Hamm AO. Brain activation and defensive response mobilization during sustained exposure to phobia-related and other affective pictures in spider phobia. Psychophysiology 2008;45:205–15. https://doi.org/10.1111/j.1469-8986.2007.00620.x.
[21] Kim AY, Jang EH, Kim S, Choi KW, Jeon HJ, Yu HY, et al. Automatic detection of major depressive disorder using electrodermal activity. Sci Rep 2018;8:17030. https://doi.org/10.1038/s41598-018-35147-3.
[22] Jaques N, Taylor S, Azaria A, Ghandeharioun A, Sano A, Picard R. Predicting students' happiness from physiology, phone, mobility, and behavioral data. Int Conference on Affective Computing and Intelligent Interaction (ACII) 2015;2015:222–8. https://doi.org/10.1109/ACII.2015.7344575.
[23] Jang E-H, Park B-J, Park M-S, Kim S-H, Sohn J-H. Analysis of physiological signals for recognition of boredom, pain, and surprise emotions. J Physiol Anthropol 2015;34:25. https://doi.org/10.1186/s40101-015-0063-5.
[24] Publication recommendations for electrodermal measurements. Psychophysiology 2012;49:1017–34. DOI: 10.1111/j.1469-8986.2012.01384.x.
[25] Posada-Quintero HF, Chon KH. Innovations in electrodermal activity data collection and signal processing: a systematic review. Sensors 2020;20:479. https://doi.org/10.3390/s20020479.
[26] Posada-Quintero, Hugo F., Bruce J. Derrick, Christopher Winstead-Derlega, Sara I. Gonzalez, M. Claire Ellis, John J. Freiberger, and Ki H. Chon. "Time-Varying Spectral Index of Electrodermal Activity to Predict Central Nervous System Oxygen Toxicity Symptoms in Divers: Preliminary Results." In 2021 43rd Annual International Conference of the IEEE Engineering in Medicine Biology Society (EMBC), 1242–45, 2021. https://doi.org/10.1109/EMBC46164.2021.9629924.
[27] Posada-Quintero HF, Kong Y, Nguyen K, Tran C, Beardslee L, Chen L, et al. Using electrodermal activity to validate multilevel pain stimulation in healthy volunteers evoked by thermal grills. American J Physiology-Regulatory, Integrative and Comparative Physiology 2020;319:R366–75. https://doi.org/10.1152/ajpregu.00102.2020.
[28] Posada-Quintero HF, Reljin N, Moutran A, Georgopalis D, Lee E-C-H, Giersch GEW, et al. Mild dehydration identification using machine Learning to assess autonomic responses to cognitive stress. Nutrients 2020;12:42. https://doi.org/10.3390/nu12010042.
[29] Posada-Quintero HF, Florian JP, Orjuela-Cañón ÁD, Chon KH. Highly sensitive index of sympathetic activity based on time-frequency spectral analysis of electrodermal activity. American J Physiology-Regulatory, Integrative and Comparative Physiology 2016;311:R582–91. https://doi.org/10.1152/ajpregu.00180.2016.
[30] Posada-Quintero HF, Bolkhovsky JB, Reljin N, Chon KH. Sleep deprivation in young and healthy subjects is more sensitively identified by higher frequencies of electrodermal activity than by skin conductance level evaluated in the time domain. Front Physiol 2017;8.
[31] Kong Y, Posada-Quintero HF, Chon KH. Real-time high-level acute pain detection using a smartphone and a wrist-worn electrodermal activity sensor. Sensors 2021;21:3956. https://doi.org/10.3390/s21123956.
[32] Posada-Quintero HF, Landon CS, Stavitzski NM, Dean JB, Chon KH. Seizures caused by exposure to Hyperbaric oxygen in rats can be predicted by Early changes in electrodermal activity. Front Physiol 2022;12.
[33] Santiago-Espada Y. The multi-attribute task battery II (MATB-II) software for human performance and workload research: a user's guide. Hampton, Virginia: National Aeronautics and Space Administration, Langley Research Center; 2011.
[34] Hossain M-B, Posada-Quintero HF, Kong Y, McNaboe R, Chon KH. Automatic motion artifact detection in electrodermal activity data using machine learning. Biomed Signal Process Control 2022;74:103483. https://doi.org/10.1016/j.bspc.2022.103483.
[35] Hossain MB, Posada-Quintero H, Chon K. A deep convolutional autoencoder for automatic motion artifact removal in electrodermal activity. IEEE Trans Biomed Eng 2022:1. https://doi.org/10.1109/TBME.2022.3174509.
[36] Kleckner IR, Jones RM, Wilder-Smith O, Wormwood JB, Akcakaya M, Quigley KS, et al. Simple, transparent, and flexible automated quality assessment procedures for ambulatory electrodermal activity data. IEEE Trans Biomed Eng 2018;65:1460–7. https://doi.org/10.1109/TBME.2017.2758643.
[37] Posada-Quintero HF, Florian JP, Orjuela-Cañón AD, Chon KH. Electrodermal activity is sensitive to cognitive stress under water. Front Physiol 2018:8. https://doi.org/10.3389/fphys.2017.01128.
[38] Wang H, Siu K, Ju K, Chon KH. A high resolution approach to estimating time-frequency spectra and their amplitudes. Ann Biomed Eng 2006;34:326–38. https://doi.org/10.1007/s10439-005-9035-y.
[39] Huang NE, Shen Z, Long SR, Wu MC, Shih HH, Zheng Q, et al. The empirical mode decomposition and the Hilbert spectrum for nonlinear and non-stationary time series analysis. Proce Royal Society of London Series A: Mathematical Physical and Eng Sci 1998;454:903–95. https://doi.org/10.1098/rspa.1998.0193.
[40] Chawla NV, Bowyer KW, Hall LO, Kegelmeyer WP. SMOTE: synthetic minority over-sampling technique. J Artif Int Res 2002;16:321–57.
[41] Breiman L. Random forests. Mach Learn 2001;45:5–32. https://doi.org/10.1023/A:1010933404324.
[42] Fisher A, Rudin C, Dominici F. All models are wrong, but many are useful: learning a variable's importance by studying an entire class of prediction models simultaneously. J Mach Learn Res 2019. https://doi.org/10.48550/arXiv.1801.01489.
[43] Hossain M-B, Kong Y, Posada-Quintero HF, Chon KH. Comparison of electrodermal activity from multiple body locations based on Standard EDA indices' quality and robustness against motion Artifact. Sensors 2022;22:3177. https://doi.org/10.3390/s22093177.